The Effect of Thermal Residual Stresses Analysis on Tetrahedral Elements Surface Structure

Kadhim Karim Mohsen

Mechanical Engineering Department

College of Engineering

Thi-Qar University

Abstract

This study investigates the effect of thermal residual stress analysis on tetrahedral elements surface structure using finite element technique. An understanding of the effects related to the thermal residual stress is necessary to improve the ability of designers to precisely predict the catastrophic behavior of the apparatuses during overhaul. Tetrahedral elements surface structure production component subjected to applied loads needs to optimize this component that is critical to the tetrahedral elements surface structure efficiency. The applied loads and resulting residual stresses under service conditions is demanded. The finite element modeling was performed. In addition, the fracture life prediction was carried out using finite element based on fatigue analysis. It was observed that the fracture was significantly influenced due to the residual stresses. The obtained result indicates that the existence residual stresses produce the shortest fatigue life for applied loads conditions. The process is one of the promising surface treatments to increase the fracture life for tetrahedral elements surface structure.

Keywords: Tetrahedral elements surface; residual Stresses; fatigue, finite element method, optimization design.

تأثير تحليل الاجهادات المتبقية الحرارية على هيكل رباعي السطوح

المستخلص

تهدف هذه الدراسة الى بحث تاثير الاجهادات المتبقية الحرارية على هيكل رباعي السطوح باستخدام طريقة العناصر المحددة حيث ان من الضروري معرفة التاثيرات الحرارية التي لها علاقة بالاجهادات المتبقية لتحسين قدرة المصممين للتنبأ بدقة سلوك المنتج للفشل اثناء الخدمة . ان الهيكل رباعي السطوح المعرض الى احمال حرارية مسلطة عليه يحتاج الى تصميم امثل لزيادة كفاءة الهيكل حيث تتطلب الاحمال المسلطة والاجهادات المتبقية اثناء ظروف الخدمة اضافة الى انه تم بناء انموذج رياضي للتنبا بعمر الكسر باستخدام طريقة العناصر المحددة معتمدة على تحليل الكسر.وبالاعتماد على نتائج

طريقة العناصر المحددة تبين ان عمر الكسر يتاثر بصورة كبيرة بالاجهادات المتبقية حيث النتائج اعطت مؤشرا على ان الاجهادات المتبقية تؤدي الى عمر اقصر للهيكل لجميع ظروف العمل وان هذه العملية هي واحدة من المعالجات لعمر الكلل لوصلات هيكل رباعي السطوح.

كلمات مرشدة:رباعي السطوح ،الاجهادات المتبقية،الكلال ، طريقة العناصر المحددة، التصميم الامثل.

1. Introduction

The use of linear tetrahedral elements facilitates the exact analytical integration of the finite element arrays, and therefore the exact evaluation of the discrete balance equation. Further, the discontinuous integration procedure let us evaluate correctly the discontinuous nature of phase-change phenomena.

The highly non-linear equation governing the problem is solved using the Newton-Raphson method, with an exact, analytically computed tangent matrix. Such an iterative method provides probably the fastest way to solve this equation. Convergence starting from initial solutions lyingout of the “attraction” zone was enforced using a line-search procedure. Therefore, it yields an improvement of the robustness of Newton-Raphson method.
Thermal results were correctly validated against an analytical solution for a non-is other malphase change problem [1].

The interaction between electricity and elasticity were analyzed using tetrahedral elements. However, these elements were too thick for thin shell or plate applications. To overcome this drawback, Tzou and Tseng (1990) proposed a ‘‘thin” piezoelectric solid element by adding three internal degrees of freedom for the vibration control of structures with piezoelectric materials. Hwang et al. (1993)employed classical laminated plate theory (CLPT) to analyze the vibration control of a laminated plate with piezoelectric sensors and actuators. Their study explored the optimal design of the piezoelectric sensors and actuators. Based on the ®rst-order shear deformation theory, Chandrashekhare and Tenneti (1995) developed a finite element model for the vibration control of laminated plates with piezoelectric sensors and actuators and analyzed the thermally induced vibration suppression of laminated plates. Robbins and Reddy (1991) presented the finite element model of a piezoelectrically actuated beam by using four deferent displacement-based one-dimensional beam theories all of which can be reduced from the generalized laminated plate theory of Reddy (1987) [2].

Previous tetrahedral schemes based on generalizations of box splines have encoded arbitrary directional preferences in their associated subdivision rules that were not reflected in

tetrahedral base mesh. Our method avoids this choice of preferred directions resulting a scheme that is simple to implement via repeated smoothing. In an extended appendix, we analyze this tetrahedral scheme and prove that the scheme generates C2 deformations everywhere except along edges of the tetrahedral base mesh. Along edges shared by four or more tetrahedra in the base mesh, we present strong evidence that the scheme generates C1 deformations [3].

The high residual compressive stress of tetrahedral amorphous carbon film deposited by the filtered vacuum arc process causes instability of the coating and substantially limits its applications. The high residual stress is a matter of particular concern for its application to micro electromechanical systems MEMSbecause the MEMS structure can be severely deformed even when very thin ta-C film is deposited. Systematic control of the residual stress has thus been one of the most important issues in ta-C coating technology. However, a decrease in the residual compressive stress is usually accompanied by the deterioration of the advantageous properties such as high hardness, optical transparency, or surface smoothness [4].

Residual stresses are known to influence a material's mechanical properties such as creep or fatigue life. Sometimes, the effect on properties is beneficial; other times, the effect is very deleterious. Therefore, it is important to be able to monitor and control the residual stresses.

Residual stresses are stresses that remain after the original cause of the stresses (external forces, heat gradient) has been removed. They remain along a cross section of the component, even without the external cause. Residual stresses occur for a variety of reasons, including inelastic deformations and heat treatment. Heat from welding may cause localized expansion, which is taken up during welding by either the molten metal or the placement of parts being welded. When the finished weldment cools, some areas cool and contract more than others, leaving residual stresses. Another example occurs during semiconductor fabrication and micro system fabrication when thin film materials with different thermal and crystalline properties are deposited sequentially under different process conditions. The stress variation through a stack of thin film materials can be very complex and can vary between compressive and tensile stresses from layer to layer.

Induction surface hardening creates a very desirable thermal residual stress state at the surface and thermal residual stress distribution below the surface. Residual stresses are always of a compressive nature and are usually present to the depth of the induction surface hardened layer. Amajordifficulty in induction surface hardening is, however, to ensure a very slight

variation in hardness and the existence of compressive residual stresses in transition areas to the hardness of the base material. By gently varying the hardness and through compressive residual stresses in the transition area, it is possible to diminish the notch effect induced by stress concentration in parts loaded by cyclic tensile stresses. Additional grinding of the induction surface hardened surface has an adverse effect on the stress state in the surface layer, since grinding always induces tensile residual stresses. By correct selection of the machining conditions and the grinding wheel, taking into account its properties, the engineer will contribute to lessening the relative grinding tensile thermal residual stress distributions which will help keep the favourablethermal residual stress state after induction surface hardening [2].

The residual stresses near the weld root and the weld toe for multi-pass welded tube-to-plates. Two different tubular joint configurations were studied; a three-pass single-U weld groove for maximum weld penetration and a two-pass fillet (no groove) welded tube-to-plates for minimum weld penetration. A 2D axi-symmetric finite element model was developed to calculate the distribution, HAZ, penetration depth and the thermal residual stress distribution for the sequentially coupled thermo-mechanical analysis. The calculated residual stresses was compared with experimental results and showed qualitatively good agreement. Torsion fatigue tests were performed in order to study crack propagation from the weld root, lower and upper weld toe in mode III. Some of the tube structures were loaded with a static internal pressure in order to separate the root crack and initiate the crack growth in mode III. Another batch was PWHT and fatigue tested, in order to study the influence of residual stresses [3].

Established methods for calculating residual stresses from the strains measured when using the slitting method give results for the stresses that exist within the depth range of the slit. Practical considerations typically limit this range to about 90-95% of the specimen thickness. Force and moment equilibrium can provide additional information that may be used to estimate the residual stresses in the “no-data” region within the remaining ligament beyond the maximum slit depth. Three different numerical methods to calculate the thermal residual stress profile over the entire specimen thickness are investigated. They are: truncated Legendre series, regularized Legendre series, and regularized unit pulses. In tests with simulated strain data and with strain data measured on a cold compressed 7050-T7452 Aluminum hand forging, the three methods gave generally similar stress results in the central region of the specimen. At small depths, where the strain sensitivity to the residual stresses is low, the two regularized calculation methods tended to give more stable results. In the area of

very large depth beyond the maximum depth of the slit, the regularized Legendre series solution generally gave the most realistic stress results [4].

Finite Element Analysis (FEA) has been carried out on a single pass butt welding model to illustrate the distortion and thermal residual stress field developed in the weldment. Thermo-elastic-plastic analysis has been used to find the residual stresses and distortion. It was found that the residual stresses and distortion values increase with of laser beam power. On the other hand, the distortion and residual stresses decrease as the speed increases. There is a reduction of thermal residual stress and distortion values as the spot diameter increases [5].

This study presents a direct analysis ,discrete and composite modeling of tetrahedral elements surface structure in three dimension detail interaction of the long-term behavior differential settlement estimation. The crack initiation and propagation result in tetrahedral elements surface structure and life-cycle prediction High-end detail analysis (crash, fatigue, fracture mechanism) caused by shear in wall.

2. Types of loads

Loads cause stresses, deformations, and displacements in structures. Assessment of their effects is carried out by the methods of structural analysis. Excess load or overloading may cause structural, and hence such possibility should be either considered in the design or strictly controlled.

Mechanical structures, such as aerospace vehicles (e.g. aircraft, satellites, rockets, space stations, etc...), marine craft (e.g. boats, submarines, etc.), and material handling machinery have their own particular structural loads and actions.

Loads can be classified as dead loads, live loads ,environmental loads, and other loads .The dead loads are static forces that are relatively constant for an extended time. They can be in tension or compression. The term can refer to a laboratory test method or to the normal usage of a material or structure.

Live loads are usually unstable or moving loads. These dynamic loads may involve considerations such as impact, momentum, vibration, slosh dynamics of fluids, etc. An impact load is one whose time of application on a material is less than one-third of the natural frequency of vibration of that material.

Cyclic loads on a structure can lead to fatigue damage, cumulative damage, or failure. These loads can be repeated loadings on a structure or can be due to vibration. The Environmental loads are act as a result of weather, topography and other natural phenomena [6].

Equation of equilibrium is given by:

$$\Delta\sigma + F = 0$$

where, Δσ is the stress variation and F is the body force. Residual stresses are calculated by using the principle of virtual work. In this method, one considers infinitesimal nodes displacements {δ} imposed onto the body. This causes external total virtual work (equal to the total internal virtual work which is defined by stresses {σ} and strains {ε}). By using FEM (finite element model), strain–displacement can be expressed briefly as follows:

$$\{\varepsilon\} = [B]\{\delta\}e$$

where, {ε} is the strain vector, [B] is the strain–displacement interpolation matrix and {δ}e is the displacement vector for an element. The nodal displacement is obtained from

$$\{\delta\}[K]^{-1}(\{R\}_T\{R\}_P)$$

where, [K] is the conductivity matrix,$\{R\}_T$,$\{R\}_P$is the resultant nodal displacements vector with respect to nodal temperature and laser beam power.

The stress-strain relationship is defined as follows:

$$\{\sigma\} = [D](\{\varepsilon_e\})$$

where, [D] is the Stiffness matrix and {εe} is the elastic strain vector. For the deformation of metals, the Von Mises yield criterion is employed and the elastic strain is given by

$$\varepsilon_e = \varepsilon - \varepsilon_{pl} - \varepsilon_{th}$$

where, ε_e is the elastic strain, ε is the total strain,$\varepsilon_{pl}$is plastic strain and$\varepsilon_{th}$is the thermal strain.

3. Parameters effect on the values of the residual stresses

Influence of some parameters on the residual stresses from quenching concentrates some important effects on the development of residual stresses from quenching: the influence of the martensitic temperature interval and the influence of the shift of the martensite start

temperature caused by thermal stresses. The influence of the location of the maximum quenching rate on the thermal residual stress pattern is also discussed.

A numerical model of the coupled elasto-plastic problem has been developed, which incorporates the influence of the thermal stresses on the martensite start temperature. It is demonstrated that the length of the martensitic temperature interval may have a significant effect on the thermal residual stress pattern. While large martensitic intervals promote compressive residual stresses at the surface, small martensitic intervals give rise to tensile residual stresses even for small thermal gradients at martensitic temperatures.

The shift of the martensite start temperature due to thermal stresses should always be incorporated in calculations because of significant effects on the thermal residual stress pattern. It is also established that during quenching, the thermal stresses always raise the martensite start temperature at the specimen surface, thus promoting non-uniform phase transformation over the cross section of the specimens

Due to the non-uniform temperature distribution during the thermal cycle, incompatible strains lead to thermal stresses. These incompatible strains due to dimensional changes associated with solidification of the weld metal, metallurgical transformations and plastic deformation, are the main sources of residual stresses and distortion [7].

4. Controlled residual stress

Avoid unknown or random thermal residual stress by forbidding quenching of low ductility, light alloy castings into water following high temperature solution treatment. Boiling water is also not permitted since it represents a negligible improvement over cold water. However, polymer quenchant or forced air-quench may be acceptable if casting stress is shown to be negligible. Planned thermal residual stress may be beneficial if designed correctly into the quenching process.

Uncontrolled residual stresses are undesirable, some designs rely on them. For example, toughened glass and pre-stressed concrete depend on thermal residual stress to prevent brittle failure. A demonstration of the effect is shown by Prince Rupert’s Drop, where a molten glass globule is quenched to produce a toughened outer layer [8].

Allthermo-mechanical manufacturing processes—such as forging, extrusion, casting, heat treatment, welding, coating, and machining—create residual stresses in industrial products. There are situations when such stresses can be beneficial and are intentionally created, for example, compressive stresses on the outer surface of a component subjected to fatigue loads, autofrettage in gun barrels, and prestressed pressure vessels; even bolted connections and prestressed concrete can be included in this category. In many other situations, however, the presence ofthermal residual stress is detrimental to the integrity of the product under service conditions. Examples in this category include: tensile stresses on the outer surface of a component subjected to fatigue loads, tensile stresses on the inner surface of an austenitic stainless steel pipe caused by welding leading to intergranular stress-corrosion cracking in boiling water reactors, interlaminar stresses in coatings leading to their spallation, premature yielding or fracture (especially in brittle materials), and part distortion or dimensional instability. The presence of residual stresses in a part is also known to affect its machinability. For these reasons, mechanical and manufacturing engineers have long been interested in understanding the source of such stresses, their control, and relief .In the case of metallic products, the selection of material is generally dictated by functional requirements such as the ability of the product to withstand service loads, resistance to wear or corrosion, and so forth. It is rare that the magnitude and distribution of residual stresses is a matter of primary consideration while selecting the material to manufacture a metallic part. The issue facing the manufacturing engineer is to control the residual stresses in the product once the material (and often the manufacturing process) has already been selected. In the case of a composite or coated product, however, minimization of residual stresses is a prime consideration while selecting the constituent materials. This article primarily deals with metallic products. A logical way to control residual stresses in a product should consist of the following steps: Understanding the fundamental sources of stress generation Identifying the parameters that can cause residual stresses in a particular manufacturing process Understanding the relative significance of each one of these parameters Experimenting with the most significant process parameters until a suitable combination is obtained that results in the desired magnitude and distribution of residual stresses If the residual stresses in the product are still higher than acceptable, the only recourse left is the use of one of the various techniques of stress relief or the inducement of a stress pattern more favorable than the original [9].

There are several techniques that are used to measure the residual stress. They can be classified as destructive and non-destructive methods. Mechanical methods or dissection uses

the release of stress and its associated strain after doing a cut, hole or crack. Nonlinear elastic methods as ultrasonic or magnetic techniques require a reference sample. X-ray diffraction is a non-destructive method which allows the measurement of thermal residual stress in isolated spots spaced distances as small as 100 micrometers Residual stresses can be sufficient to cause a metal part to suddenly split into two or more pieces after it has been resting on a table or floor without external load being applied. While this is not a common occurrence, experienced people in the metal working industry have witnessed this phenomenon. While there may be additional factors causing this to occur residual stresses explain these occurrences[10].

5. Residual stresses measurement methods

The stress is an extrinsic property, which cannot be directly measured. All the methods adopted to measure the residual stresses need the measurement of some intrinsic property, such as the strain, the load and area, and after the stress can be calculated.

Possible methods of calculation

- Mechanical methods (controlled hole drilling)
- nonlinear methods (ultrasonic and magnetic techniques)
- diffract to metric methods

Thermal residual stresses are primarily due to differential expansion when a metal is heated or cooled. The two factors that control this are thermal treatment (heating or cooling) and restraint. Both the thermal treatment and restraint of the component must be present to generate residual stresses [11].

6. Analysis of residual stresses

Residual stresses are known to influence materials mechanical properties such as creep or fatigue life. Sometimes, the effect on properties is beneficial; other times, the effect is very deleterious. Therefore, it is important to be able to monitor and control the residual stresses.

Two different techniques are commonly used for measuring the residual stresses. The most popular technique is a special type of X-ray diffraction (known as the $\sin^2\psi$method), which is used to measure the stresses in fine grained crystalline materials. An alternate method, the

hole drilling method, is most often used when the X-ray technique is not appropriate. Each method, along with its advantages and disadvantages, is described in this note.

7. The X-ray diffraction method

The $\sin^2\psi$method is a sensitive and accurate technique to measure residual stresses in a fine grained, polycrystalline material. As shown in Figure(1), the position of a diffraction peak will shift as the sample is rotated by an angle ψ.

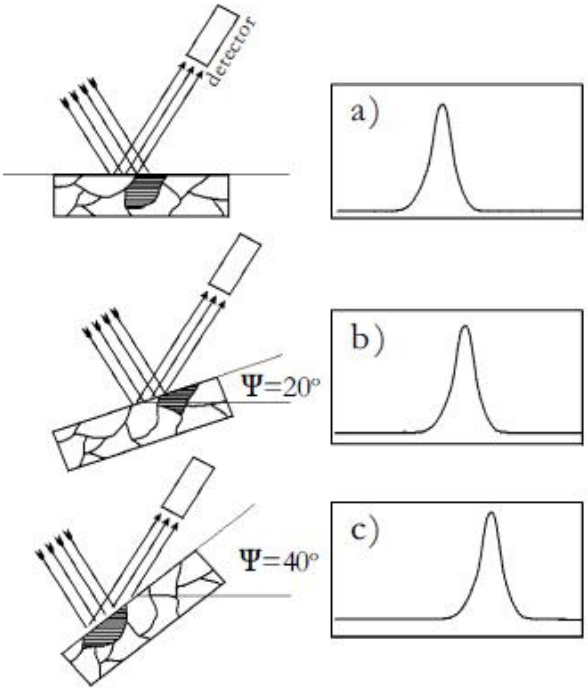

Figure (1). Shift of diffraction peak with change in Q value. Note that as Q increases in b) and c) above, the position of the diffraction peak shifts further and further away from its usual position in a).

The magnitude of the shift will be related to the magnitude of the residual stress. Thus, if there is no residual stress, the shift will be zero. The relationship between the peak shift and the residual stress σ is given by

$$\sigma = \frac{E}{(1+\upsilon)sin^2\psi}\frac{d_n - d_o}{d_o} \qquad (13)$$

where E is Young.s modulus, υis poison's ratio, ψis the tilt angle, and di are the "d" spacings measured at each tilt angle. If there are no shear strains present in the sample, the "d" spacings would change linearly with $\sin^2\psi$ and a least squares fit to the curve (for multiple values of ψ) would give σ. However, if shear strains are present, a splitting of the plot will occur and the

analysis is more complicated. Finally, if the sample is rotated in-plane, it is possible to determine the principal stresses and their directions.

8. The hole drilling method

There are many situations where X-ray diffraction is not useful for measuring residual stresses. These include non-crystalline materials, large grained materials, nanomaterials, textured, or heavily deformed metals. In these cases, other mechanical methods such as the hole-drilling method are used. The hole-drilling method (ASTM Standard E837) relies on stress relaxation when a hole is drilled into the center of a rosette strain gage such as that shown below. When the material is removed by drilling, the extent of the strain relief is monitored by the gages and the direction and magnitude of the principal stresses can be calculated.

Figure(2). Rosette gage (Magnification: 4x)

A special high speed air turbine drill (shown above) is used to first locate the drill to within 0.001. of the rosette center and then to remove material to a controlled depth. At each depth increment, the strain relief on each of the gages is measured and converted into stress. As subsequent material removals occur, the stress distribution as a function of depth can be estimated. The hole drilling method is used in those situations where the residual stress is relatively uniform over the drilling depth. Thus, it is not intended for situations where the residual stress is superficial.

The accuracy of the hole drilling method is directly related to the ability of locating the hole accurately in the center of the rosette. As an example, if the hole is no more than 0.001. off center, the residual strain error is less than 3%. In practice, the location accuracy is better than this, so the overall accuracy in residual stress measurements is quite good. Another important consideration in this method is the ability to drill the relief hole so as not to

introduce new stresses. This is best achieved in hard materials by use of a high-speed turbine drill which avoids excessive rubbing of the cutting surface against the hole wall. As a result of careful design of the tool, the holes have f lat bottoms and straight walls as required by ASTM E837. The hole drilling method has many advantages, but it also has many disadvantages. Of particular concern is that the method is valid only up to about 50% of the yield strength of the test material. Thus, great care has to be exercised when selecting testing methods [12].

The aim of the present study is therefore to propose a further development to facilitate and accelerate geometry acquisition modification during the fabrication of FE models of restorations.

9. Finite element method analysis

Finite element method analysis is a simulation technique which evaluates the behavior of components, equipment and structures for various loading conditions including applied forces, pressures and temperatures. Thus, a complex engineering problem with non-standard shape and geometry can be solved using finite element analysis where a closed form solution is not available. The finite element analysis methods result in the stress distribution, displacements and reaction loads at supports etc. for the model. Finite element analysis techniques can be used for a number of scenarios e.g. Design optimization, material weight minimization, shape optimization, code compliance etc

Most engineering materials have linear stress-strain relationships [12]. These relationships can be expressed for of homogenous material as

$$\sigma = E\gamma \tag{1}$$

$$\tau = G\gamma \tag{2}$$

These relationships are known as Hooke s Law, , where E is the modulus of elasticity, the ε are the normal strains, the σ are the normal stresses, G is the modulus of rigidity, the σij are the shearing stresses, and the γ are the shearing strains. In order to express the strain components γ in terms of the stress components, we use the principle of superposition, which states that the effect of a given combined loading on a structure can be obtained by determining separately.

For general complex isotropic tetrahedral elements surface structure with mass matrix [m_i], stiffness matrix [k_{ij}], damping matrix [c_i], and column matrix of external forces [pj]

Displacement function

$$u_{ij}(x) = c_{ij}\phi_{ij}(x) \tag{3}$$

$$\varepsilon = \frac{\partial u_{ij}(x)}{\partial x} \tag{4}$$

The residual stresses;

$$\tau = \frac{k_{ij}}{A_{ij}}\gamma + \delta_{ij}\varepsilon'_{ij} \tag{5}$$

The Generalized stiffness coefficient is

$$k_{ij} = \int_0^l E_i I_i \phi''^2_{ij} dx + k_i \phi_i^2 \tag{6}$$

The proportional generalized damping coefficients, damping ratios, damped natural frequencies and damped period the in the ith mode can be obtained from the relation:

$$C_i = \int_0^l C_i \phi_{ij}^2 dx \tag{7}$$

$$C_i = 2\zeta_i m_{ij}\omega_i$$

$$C_{C_{ri}} = 2m_{ij}\omega_i$$

$$\omega_{di} = \omega_i\sqrt{1-\zeta_i^2} \tag{8}$$

$$\tau_d = \frac{2\pi}{\omega_{di}}$$

where A_{ij} = cross-sectional area of tetrahedral elements surface structure

$A_{ij} = b_{ij}\, t_i$

b_{ij} = Width of tetrahedral structure elements

t_i = Thickness of tetrahedral structure elements

To find the tetrahedral elements stiffness matricesk_{ij}

$$[K]^{x=1,2,3,\dots} = \begin{bmatrix} k_{11}^{x} & k_{12}^{x} & k_{13}^{x} & k_{14}^{x} & k_{15}^{x} & k_{16}^{x} \\ k_{21}^{x} & k_{22}^{x} & k_{23}^{x} & k_{24}^{x} & k_{25}^{x} & k_{26}^{x} \\ k_{31}^{x} & k_{32}^{x} & k_{33}^{x} & k_{34}^{x} & k_{35}^{x} & k_{36}^{x} \\ k_{41}^{x} & k_{42}^{x} & k_{43}^{x} & k_{44}^{x} & k_{45}^{x} & k_{46}^{x} \\ k_{51}^{x} & k_{52}^{x} & k_{53}^{x} & k_{54}^{x} & k_{55}^{x} & k_{56}^{x} \\ k_{61}^{x} & k_{62}^{x} & k_{63}^{x} & k_{64}^{x} & k_{65}^{x} & k_{66}^{x} \end{bmatrix} \quad (9)$$

For the first 4 trusses tetrahedral elements surface structure stiffeners

$$[K] = \begin{bmatrix} k_{11}^{1} & k_{12}^{1} & k_{13}^{1} & k_{14}^{1} & 0 & 0 & 0 & 0 & 0 & 0 & 0 & 0 & 0 & 0 & 0 & 0 \\ k_{21}^{1} & k_{22}^{1} & k_{23}^{1} & k_{24}^{1} & & & & & & & & & & & & 0 \\ k_{31}^{1} & k_{32}^{1} & k_{33}^{1} & k_{34}^{1} & & & & & & & & & & & & 0 \\ k_{41}^{1} & k_{42}^{1} & k_{43}^{1} & k_{44}^{1} & & & & & & & & & & & & \\ & & & & k_{11}^{2} & k_{12}^{2} & k_{13}^{2} & k_{14}^{2} & & & & & & & & \\ & & & & k_{21}^{2} & k_{22}^{2} & k_{23}^{2} & k_{24}^{2} & & & & & & & & \\ & & & & k_{31}^{2} & k_{32}^{2} & k_{33}^{2} & k_{34}^{2} & & & & & & & & \\ & & & & k_{41}^{2} & k_{42}^{2} & k_{43}^{2} & k_{44}^{2} & & & & & & & & \\ & & & & & & & & k_{11}^{3} & k_{12}^{3} & k_{13}^{3} & k_{14}^{3} & & & & \\ & & & & & & & & k_{21}^{2} & k_{22}^{3} & k_{23}^{3} & k_{24}^{3} & & & & \\ & & & & & & & & k_{31}^{3} & k_{32}^{3} & k_{33}^{3} & k_{34}^{3} & & & & \\ & & & & & & & & k_{41}^{3} & k_{42}^{3} & k_{43}^{3} & k_{44}^{3} & & & & \\ & & & & & & & & & & & & k_{11}^{4} & k_{12}^{4} & k_{13}^{4} & k_{14}^{4} \\ & & & & & & & & & & & & k_{21}^{4} & k_{22}^{4} & k_{23}^{4} & k_{24}^{4} \\ & & & & & & & & & & & & k_{31}^{4} & k_{32}^{4} & k_{33}^{4} & k_{34}^{4} \\ & & & & & & & & & & & & k_{41}^{4} & k_{42}^{4} & k_{43}^{4} & k_{44}^{4} \end{bmatrix} \quad \dots (10)$$

using over labia method

$$[K] = K_1 + K_2 + K_3 + K_4 \quad (11)$$

$$[K] = \begin{bmatrix} k_{11}^1 & k_{12}^1 & k_{13}^1 & k_{14}^1 & & & & & & & & \\ k_{21}^1 & k_{22}^1 & k_{23}^1 & k_{24}^1 & & & & & & & & \\ k_{31}^1 & k_{32}^1 & k_{33}^1+k_{11}^2 & k_{34}^1+k_{12}^2 & k_{13}^2 & k_{14}^2 & & & & & & \\ k_{41}^1 & k_{42}^1 & k_{43}^1+k_{21}^2 & k_{44}^1+k_{22}^2 & k_{23}^2 & k_{24}^2 & & & & & & \\ & & k_{31}^2 & k_{32}^2 & k_{33}^2+k_{11}^3 & k_{34}^2+k_{12}^3 & k_{13}^3 & k_{14}^3 & & & & \\ & & k_{41}^2 & k_{42}^2 & k_{43}^2+k_{21}^2 & k_{44}^2+k_{22}^3 & k_{23}^3 & k_{24}^3 & & & & \\ & & & & k_{31}^3 & k_{32}^3 & k_{33}^3+k_{11}^4 & k_{34}^3+k_{12}^4 & k_{13}^4 & k_{14}^4 & & \\ & & & & k_{41}^3 & k_{42}^3 & k_{43}^3+k_{21}^4 & k_{44}^3+k_{22}^4 & k_{23}^4 & k_{24}^4 & & \\ & & & & & & k_{31}^4 & k_{32}^4 & k_{33}^4 & k_{34}^4 & & \\ & & & & & & k_{41}^4 & k_{42}^4 & k_{43}^4 & k_{44}^4 & & \end{bmatrix}$$

.. (12)

10.Operating conditions

The model of surface structure used in the study is shown Figure(3)

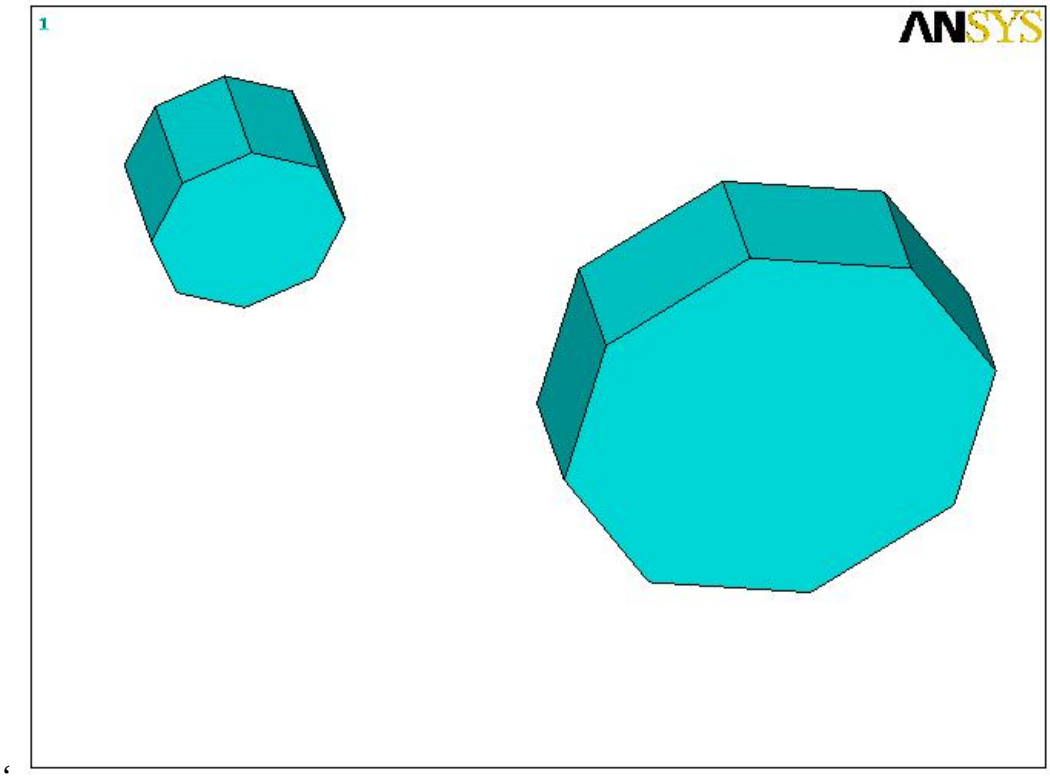

Figure(3) Model of surface structure used in the study.

The thermal residual stress in the machined layer under the assumption of homogenous material, the heat conduction equation of two dimensional field is given as [13]:

$$C_p \frac{\partial T}{\partial t} = \frac{\partial}{\partial x}\left(\lambda \frac{\partial T}{\partial x}\right) + \frac{\partial}{\partial y}\left(\lambda \frac{\partial T}{\partial y}\right) + Q \quad (13)$$

where C_p is the specific heat of the work, t the element thickness, λ the heat conductivity, the temperature T and Q the generated heat. It is assumed as well that the heat comes only from the boundary and that no heat source exists inside the material.

11.Modeling of problem

The shape function for tetrahedral elements surface structure is assumed to be linear in the finite element in the following form:

$$\phi = c_1 + c_2 x + c_3 x^2 + c_4 x^3 \quad (14)$$

as for the tetrahedral element taken in continuum as shown in Fig. (3), C_1,C_2,$C_3$and C_4 are determined by substituting$x_1, x_2, x_3, x_4, y_1, y_2, y_3, and\ y_4$

Equation (14) can be written as

$$\phi = \frac{1}{2S}\{\langle y_{43}(x - x_3) - x_{43}(y - y_3)\rangle T_1 + \langle -y_{42}(x - x_4) - x_{42}(y - y_4)\rangle T_2 + \langle y_{31}(x - x_3) - x_{31}(y - y_3)\rangle T_3 + \langle y_{21}(x - x_1) - x_{21}(y - y_{12})\rangle T_4\} \quad (15)$$

where $T_1, T_2, T_3 and\ T_4$are the temperature at the nodes and Sis the boundary surface of the tetrahedral structure

$$x_{ij} = x_i - x_j \quad and \quad y_{ij} = y_i - y_j$$

The tetrahedral structure surface region is divided into finite number of element rectangular in shape as shown in Figure(4)connected at their four nodes for plane stress and along inters elements boundaries, equilibrium and compatibility must be satisfied at each node and along the boundaries between the elements.

The general form for the thermal residual stress [14]

$$\sigma_{ij} = -\frac{E \propto \Delta T}{(1 - \upsilon)} \quad (16)$$

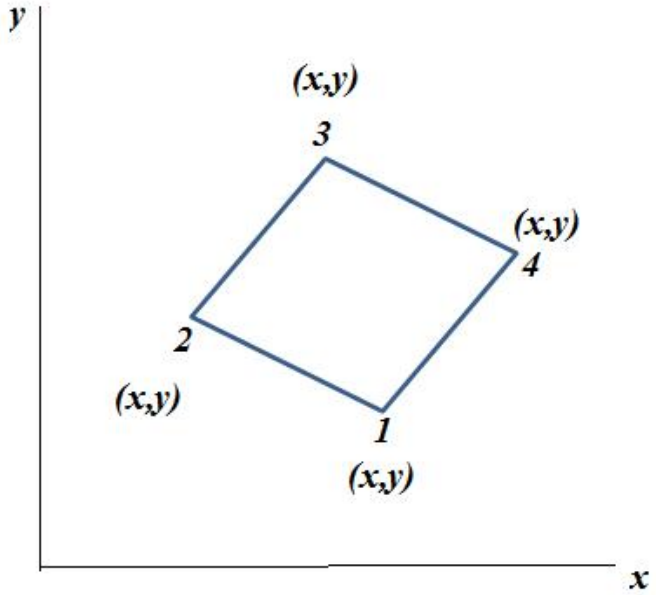

Figure (4).A plane stress of tetrahedral structure surface region divided into finite elements.

Therefore the division of a three-dimensional region into tetrahedral elements of the continuous structure can be shown in Figure(5)

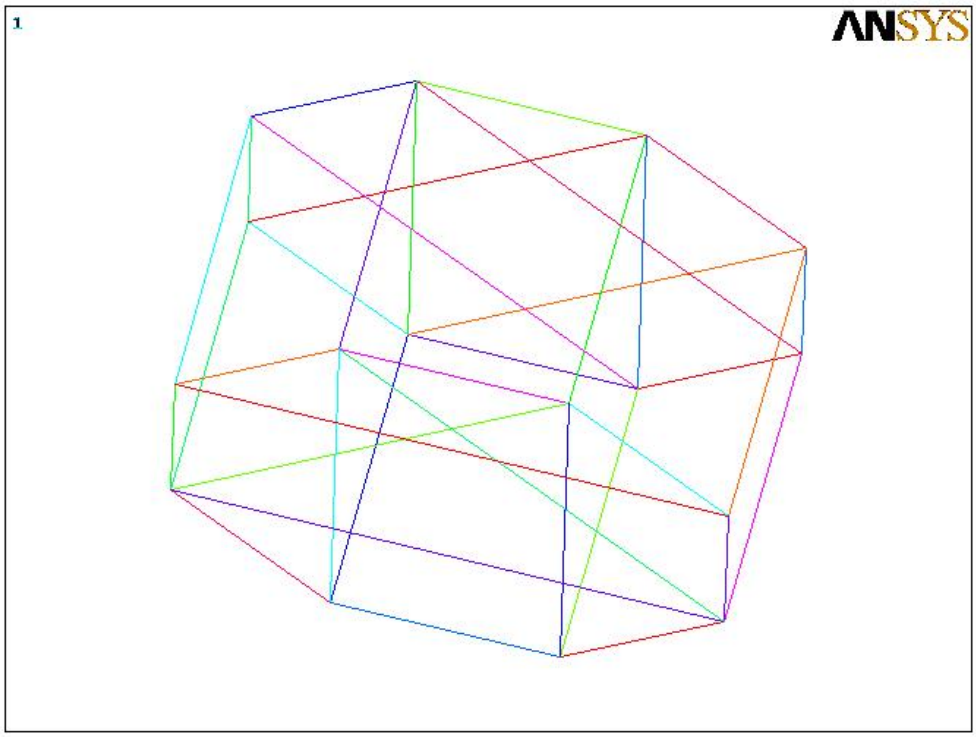

Figure(5). Division of a three-dimensional region into tetrahedral elements .

Fracture life prediction can be obtained from the previous equations as follows:

$$N_f = c/\mu A_{ij} D \sum_{i=1}^{n} \sum_{j=1}^{n} k_{ij} F_i \phi \qquad (15)$$

12.Results and discussion

For various loading conditions investigated, the thermal residual stress analysis results for the tetrahedral elements surface structure were checked against the allowable stresses. The stress and displacement results were found to be suitable per structural engineering practices.

Thermal residual stress can be determined from the tetrahedral geometry of the structure and the distribution of strains and stresses combination set up during the operating conditions. For temperature changes leading to thermal expansion cause thermal loads then residual stresses are caused by the thermal loading that occurs when hot tetrahedral elements surface structure metal is cooled metal. Successive cooling causes thermal, plastic, and transformation of stresses strains to format the material, and these strains give rise to residual stress.

By using the Ansys program to study the output graphs for present work as follows:

Figure(6) and (7) show the application of equation (16) which explain the relationship between the residual stresses after temperature change where the residual stresses of the heated element is higher than the lower one.

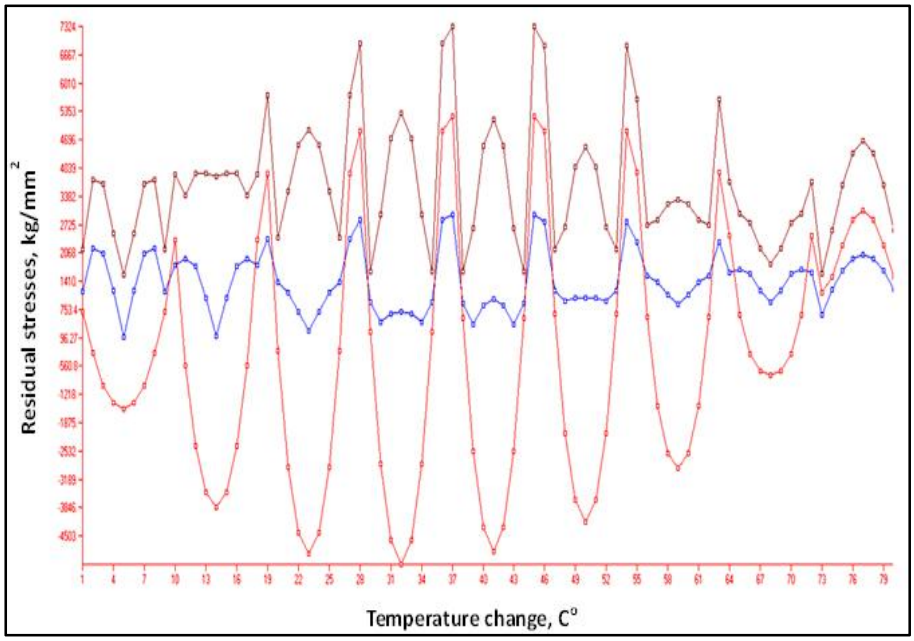

Figure (6). Residual stresses of the tetrahedral structure.

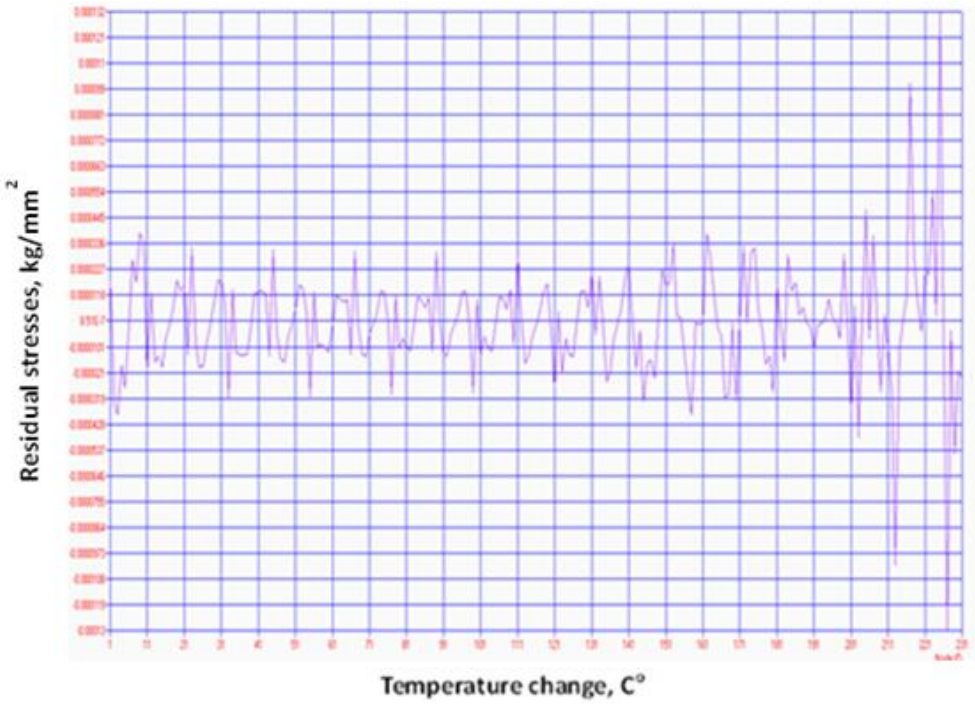

Figure(7). Residual stresses for one element.

Figure (8) show the Variation of Residual stresses of the tetrahedral structure with thickness ,The strengths of the truss prevent the residual stresses to penetrable into the truss grains, and decelerates away from the boundary.

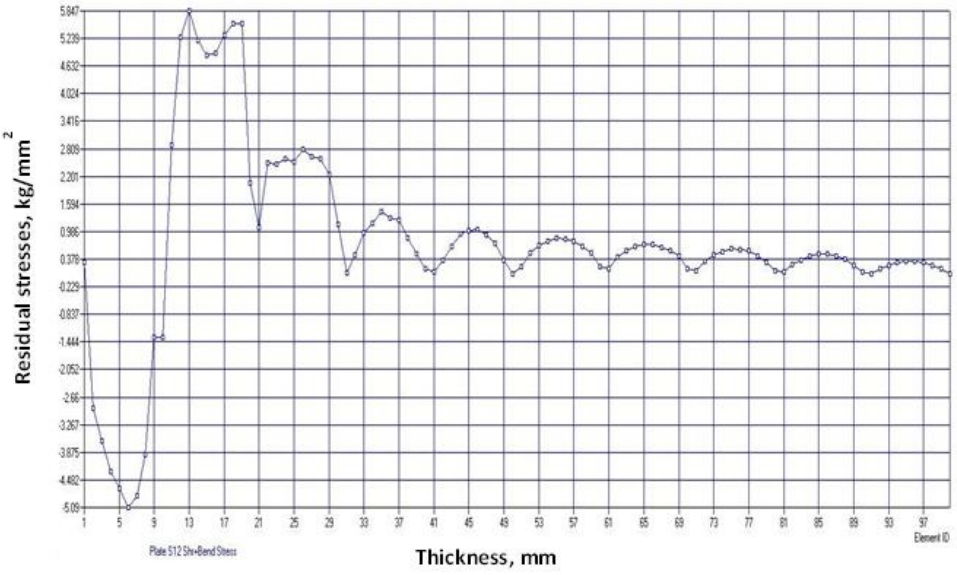

Figure(7). Variation of Residual stresses of the tetrahedral structure with thickness.

Figure(9) shows the stress distribution along the tetrahedral elements surface with mode shape, it can be seen that the higher modes show the largest stressed of the surface,

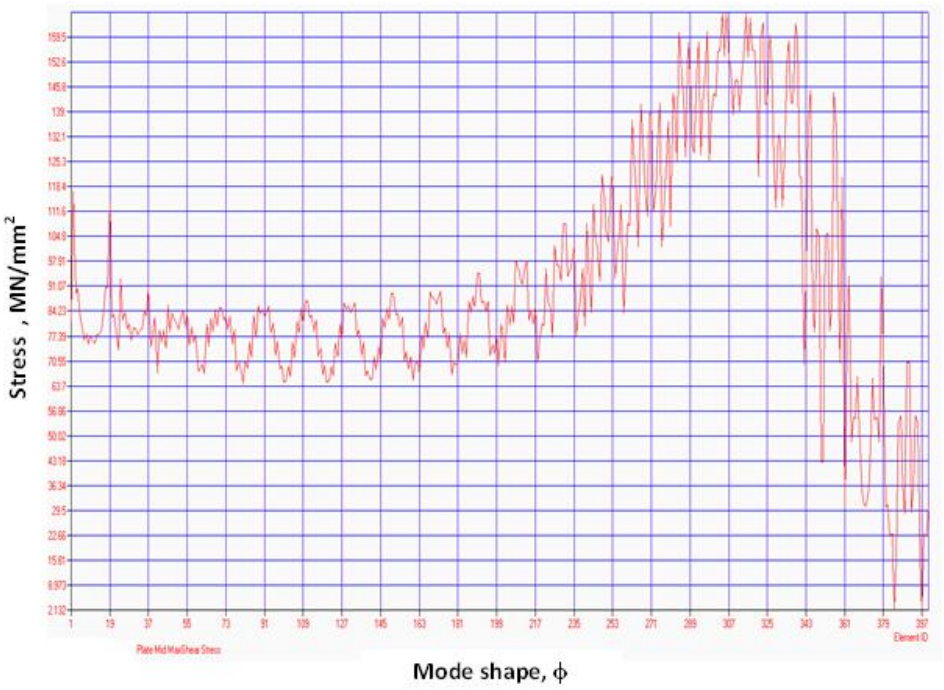

Figure(9). Stress distribution for different mode shapes.

The weakness of the truss allows the residual stresses to into the truss grains, but accelerates the residual stresses away from the boundary. Figure(10) indicate that the longer fracture life is in the higher stiffness grain boundaries , lighter damping.

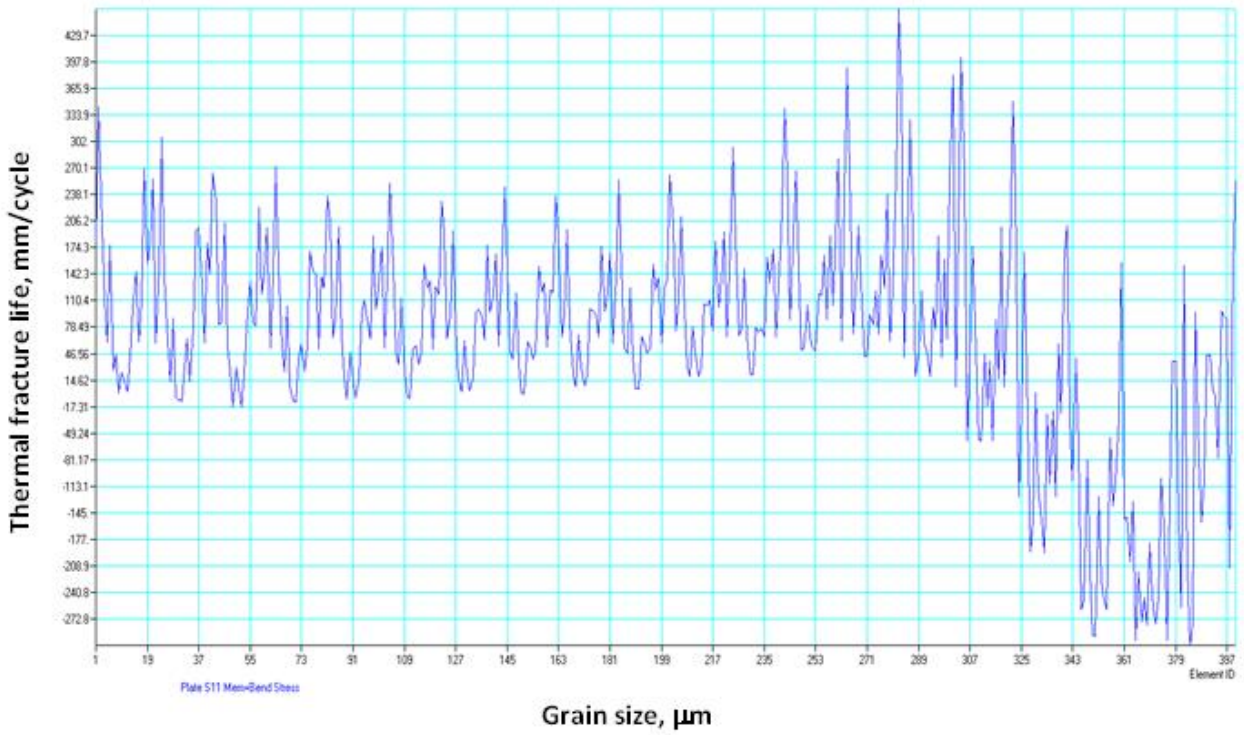

Figure (10). Thermal fracture life.

13.Conclusions

The investigation of tetrahedral elements surface structure change and the residual stress with respect to thermal deformation are studied which can be summarized as follow:

1. The thermal residual stress in the tetrahedral elements surface structure is investigated using finite element method
2. Residual stress distribution shows that tetrahedral elements surface structure is tension outward the surface and in compression inward
3. The thermal residual stress inversely increased from the elastic to plastic transition element
4. Cracks is most effective in the plastic deformation were the stress concentration is higher
5. The longer fracture life is in the higher stiffness grain boundaries, lighter damping.
6. The strengths of the truss prevent the residual stresses to penetrable into the truss grains, and decelerate away from the boundary.
7. The residual stress of the heated element is higher than the lower one.

14. References

[1] A. Anca, A. Cardona, and J.M. Risso, 3D-THERMO-MECHANICAL SIMULATION OF WELDINGPROCESSES, Universidad Nacional del Litoral–CONICETGuemes 3450, 3000, Santa Fe, Argentine .

[2]X.Q. He, T.Y. Ng, S. Sivashanker, K.M. Liew , Active control of FGM plates with integrated piezoelectricsensors and actuators, Centre for Advanced Numerical Engineering Simulations, School of Mechanical and Production Engineering, Nanyang TechnologicalUniversity, Nanyang Avenue, Singapore 639798, Singapore .

[3]S. Schaefer J. Hakenberg J. Warren, Smooth Subdivision of Tetrahedral Meshes, Eurographics Symposium on Geometry Processing (2004) R. Scopigno, D. Zorin, (Editors), Rice University .

[4]Tae-Young Kim, Churl Seung Lee,Young Jin Lee,and Kwang-Ryeol Lee,Reduction of the residual compressive stress of tetrahedral amorphous carbon film by Ar background gas during the filtered vacuum arc process, Future Technology Research Division, Korea Institute of Science and Technology, P.O. Box 131, Cheongryang, Seoul 136-791, Korea,2007 .

[5].J Grum (2002), Analysis of residual stresses in main crankshaft bearings after induction surface hardening and finish grinding, Faculty of Mechanical Engineering, University of Ljubljana, Asfkercfeva 6, 1000 Ljubljana, Slovenia .

[6]Avallone, E.A., and Baumeister, T., ed. Mark's Standard Handbook for Mechanical Engineers (10th ed.). McGraw-Hill. pp. 11–42. ISBN 0-07-004997-1.2002 .

[7] Z. Barsoum (2007),Residual stress analysis and fatigue of multi-pass welded tubular structures, Royal Institute of Technology, Department of Aeronautical and Vehicle Engineering, Teknikringen 8, 100 44 Stockholm, Sweden .

[8] Gary S. Schajer(2006), Residual Stress Solution Extrapolation for the Slitting Method using Equilibrium Constraints, Department of Mechanical Engineering, University of British Columbia, Vancouver, Canada.

[9] M T Todinov (1999), Influence of some parameters on the residual stresses from quenching, School of Metallurgy and Materials, The University of Birmingham, Birmingham, UK .

[10]Georgeta Apostol and Gheorghe Solomon (2012), parameters influence on the residual stress and distorsionat laser weld using finite element analysis, U.P.B. Sci. Bull., Series D, and Vol.74.

[11] Chandra, U.(1993), Control of Residual Stresses, ASM handbook, Vol. 20 (Materials Selection and. Design). ASM International, New Jersey.

[12] Khaled A. Alhazza (2002), Nonlinear Vibrations of Doubly Curved Cross-Ply Shallow Shells, Dissertation submitted to the Faculty of the Virginia Polytechnic Institute and State University .

[13] Chaudhury, G.K. and W.D. Dover (1985), Fatigue analysis of offshore platforms subjected to seawave loading. International Journal of Fatigue .

[14] ã H & M Analytical Services, 2002, Analysis of Residual Stresses Inc.

[15] Van Hulle, F.J. (1991), Wind energy: Technology and implementation. Proceeding of the European Conference, Amsterdam, Netherlands.

[16] Kozo Kishi and Hiroshi Eda,(1971), Analysis of the Structure and Thermal Residual Stress In the Machined Surface Layer by Grinding, University, Utsunomiya, Japan.

[17] T.L. Becker Jr. b, R.M. Cannon a, R.O. Ritchie, (1999) , An approximate method for residual stress calculation in functionally graded materials, University of California, Berkeley, USA .

15. Notations

List of Symbols

A cross-sectional area (mm^2)

c crack size (μm)

D grain diameter (mm)

E Modulus of elasticity (N/m^2)

G Modulus of rigidity (N/m^2)

N_f Fracture life (mm/cycle)

σ Normal stresses (N/m^2)

τ Shearing stresses (N/m^2)

ε Normal strains (dimensionless)

γ Shearing strains (dimensionless)

μ Coefficient of friction (dimensionless)

δ_{ij} Kroneker delta (dimensionless)

C_p Specific heat of the work ($cal/g.C^o$)

t Element thickness (mm)

λ Heat conductivity ($cal/cm.sec.C^o$)

T Temperature (C^o)

Q Generated heat.(C^o)

α Thermal expansion coefficient ($1/C^o$)

υ Poison's ratio (dimensionless)